Proceedings of the 11th International Conference on Structures in Fire

Editors: David Lange, Cristian Maluk, Kang Hai Tan, Dong Zhang, Yao Zhang, Julian Mendez Alvarez, Juan Hidalgo, Felix Wiesner, Martyn Mclaggan, Abdulrahman Zaben, Wenxuan Wu, Hangyu Xu

UQ Fire

THE UNIVERSITY OF QUEENSLAND
AUSTRALIA
CREATE CHANGE

NETZSCH
Proven Excellence.

afac

omnii
Consulting Fire Engineers

Proceedings of the 11th International Conference on Structures in Fire

Hosted by The University of Queensland

Proceedings of the 11th International Conference on Structures in Fire
(SiF 2020)

Hosted by The University of Queensland

30 November to 2 December 2020

Editors: David Lange, Cristian Maluk, Kang Hai Tan, Dong Zhang, Yao Zhang, Julian Mendez Alvarez, Juan Hidalgo, Felix Wiesner, Martyn Mclaggan, Abdulrahman Zaben, Wenxuan Wu, Hangyu Xu

Published by The University of Queensland, Australia © 2020

ISBN: 978-1-74272-343-3

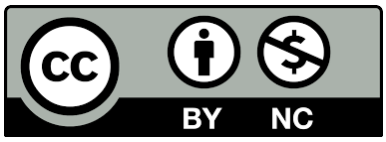

Sponsored by:

Organised by:

UQ Fire

THE UNIVERSITY OF QUEENSLAND
AUSTRALIA
CREATE CHANGE

THE UNIVERSITY OF MELBOURNE

QUT

RMIT UNIVERSITY

IFFE

UC UNIVERSITY OF CANTERBURY
Te Whare Wānanga o Waitaha
CHRISTCHURCH NEW ZEALAND

TABLE OF CONTENTS

Composite structures

Concrete structures

SiF 2020 – The 11th International Conference on Structures in Fire
The University of Queensland, Brisbane, Australia, 30th November - 2nd December, 2020

FIRE FRAGILITY CURVES FOR STEEL PIPE-RACKS EXPOSED TO LOCALISED FIRES

Jérôme Randaxhe[1], Olivier Vassart[2], Nicola Tondini[3]

ABSTRACT

This paper proposes a new method to build a probabilistic fire demand model (PFDM) to investigate the structural behaviour of a steel pipe-rack located within an industrial installation and exposed to a localised fire. The PFDM will serve to develop fire fragility functions to be used either in a fire risk assessment or in a fully probabilistic structural fire engineering (PSFE) framework. The cloud analysis (CA) was exploited to build a PFDM based on different engineering demand parameters (EDP) – intensity measures (IM) pairs. In particular, the analysis was applied to a prototype steel pipe-rack integrating an industrial plant in Italy. In order to cover a wide range of plausible fire scenarios and to introduce uncertainties in the fire model, 539 fire scenarios were examined by varying the fire diameter, the fire-structure distance and the fuel. The selection of the fire diameters was based on parametric analyses quantifying liquid flow through orifices and pipes. The thermal impact of the pool fires on the structure was analysed using the LOCAFI localised fire model and the thermo-mechanical response of the pipe rack was evaluated by means of finite element analysis. Based on the structural analysis outcomes, it was found that the interstorey drift ratio (ISDR) – maximum average heat flux impinging the structure (HF_{avg}) EDP-IM pair was the most efficient. Moreover, it has to be noted that for this type of case study, the CA revealed to be a suitable and versatile tool to build a PFDM.

Keywords: probabilistic fire demand model; cloud analysis; pool fires; LOCAFI model; fire fragility functions; steel pipe-rack structure

1 INTRODUCTION

In industrial and petrochemical plants, piping systems are used to transport flammable material, liquid or gas fuel, on long distances. They are usually supported by pipe-rack steel structures, passing between other industrial components, e.g. tanks, distillation tower, etc. These structures usually unprotected due to their significant length, are components among the most exposed to natural hazards, such as earthquakes, hurricanes or tsunamis. It appears in plants that under certain conditions, these events can trigger severe structural damages, leading a pipe or a tank to lose its containment. Furthermore, petrochemical plants are locations where a releasing flammable material is more likely to ignite than anywhere else due to activities and operations taking place in industrial environments. Even if the probability of occurrence is low, the consideration of such scenarios cannot be ignored, given their catastrophic consequences. Numerous studies have recently highlighted the exposure of petrochemical plants, piping systems to natural hazards generating technological issues, also named NaTech events. Among the wide research work which has been undertaken, Zheng and Chen [1] investigated storage tank fire accidents due to maintenance and management problems. Chan and Lin [2] reviewed 242 accidents involving storage tanks and analysed their causes to

[1] Research Engineer, Global R&D Center of ArcelorMittal, Esch-sur-Alzette, Luxembourg
e-mail: jerome.randaxhe@arcelormittal.com
[2] Chief Executive Officer Steligence at ArcelorMittal, Luxembourg
e-mail: olivier.vassart@arcelormittal.com
[3] Assistant Professor, Department of Civil, Environmental and Mechanical Engineering, University of Trento, Italy
e-mail: nicola.tondini@unitn.it, ORCID: https://orcid.org/ 0000-0003-2602-6121

https://doi.org/10.14264/e23c9a6

identify that 85% of accidents impacting petrochemical facilities are due to fires and explosions. Pantousa [3] investigated the behaviour of steel storage tanks when exposed to the thermal radiation from surrounding burning tanks. Numerous seismic analyses were performed on petrochemical piping systems and their support structure by Paolacci et al. [4–8].

Specifically, this work adopts a performance-based approach to investigate the thermo-mechanical response of a steel pipe-rack subjected to a number of meaningful fire scenarios, characterised by a pool fire located beside it, with the aim to build a probabilistic fire demand model from which deriving fire fragility functions. For that purpose, a pool fire model has to be selected, allowing the simulation of a burning tank resulting from leakage and loss of containment. It is worth pointing out that the governing heat transfer mechanism of a localised fire impacting a structure that is not engulfed into the fire, is radiation. In this respect, the LOCAFI model, developed in the framework of a European research project was exploited. [9–14].

Fragility functions are convenient tools when decisions are to be taken in structural design considering uncertainties. More specifically, for a given structure exposed to fire, a fragility function computes the probability that a structure reaches a predefined damage state (e.g. beam deflection level, interstorey drift ratio, critical temperature, …) depending on an intensity measure characterising the fire (e.g. fire load, fire geometry, …). There are few research works addressing the development of fragility functions in fire field. In particular, Gernay et al. [15,16] proposed a methodology to define fire fragility functions for a steel building exposed to compartment fires considering different fire loads. If this approach is relevant for buildings intended for offices and dwellings, it cannot be applied for a steel pipe-rack exposed to a localised fire. Lange et al. [17] and Shrivastava et al. [18] modified and adapted to fire engineering the widely used Performance-Based Earthquake Engineering (PBEE) approach from the Pacific Earthquake Engineering Research Center (PEER) probabilistic framework [19]. The use of fragility functions, considering efficient intensity measures to characterise the fire severity, allows the mitigation of fire risks when petrochemical plants are designed. However, there is a lack of work related to the study of probabilistic fire demand models relative to the structural fire behaviour of supporting structures in industrial plants.

2 CASE STUDY: PROTOTYPE STEEL PIPE-RACK

2.1 Description of the structure

The prototype steel pipe-rack considered for this work is defined in Figure 1. That structure is inspired from a reference steel pipe-rack operational in an existing petrochemical plant located in Italy. The structure is composed of several steel frames with rigid beam-to-column joints and pinned column-base joints in the transversal direction, whose distance from each other is 6 m; whereas, in the longitudinal direction, the structure is braced, with repeated modules composed of seven bays and only one endowed with bracings. Horizontal braces are used to limit relative displacements between the frames and the pipe supports. For the interest of the analyses addressed in this paper, only the supporting steel pipe-rack was considered while the structural contribution of the piping system was neglected. Furthermore, since a pipe-rack is, by definition, a structure intended for carrying pipes on kilometres, it was decided to focus the analyses on a limited and regular part. The steel grade is an S275. The columns are HEA 340, the longitudinal beams are HEA 200 and the transversal beams are HEA- and HEB 300 steel profiles, respectively. The self-weight of the pipe and their content is evaluated to 75 kN/m. This load corresponds to a pipe arrangement as depicted in Figure 1(d), considering 22” DN550 SCH140 pipes characterised by a diameter of 559 mm with a wall thickness of 47 mm, and filled with a fuel with density equal to 780 kg/m^3. The horizontal load is equal to 2 kN/m, considering the friction of the pipes, that are uniformly distributed on the transversal beams. Vertical contingency operating point loads of 15 kN and horizontal contingency friction point loads of 7.5 kN are applied at mid-span of the longitudinal beams. Wind loads acting on the structure are not considered during the fire. The loads applied on the pipe-rack are detailed in Figure 2. It has to be noted that this load combination represents about 50% of the structure vertical bearing capacity.

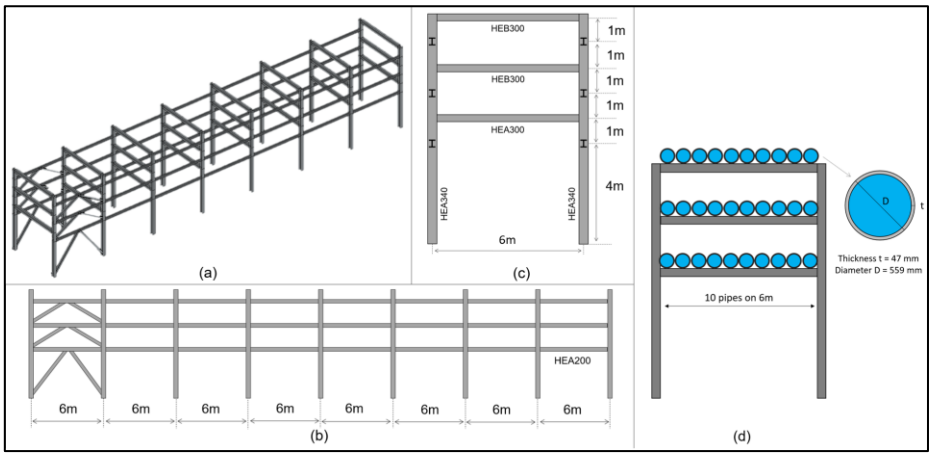

Figure 1. Prototype steel pipe-rack: (a) 3D view; (b) Longitudinal view; (c) Transversal view; (d) 22" DN550 SCH140 pipe arrangement

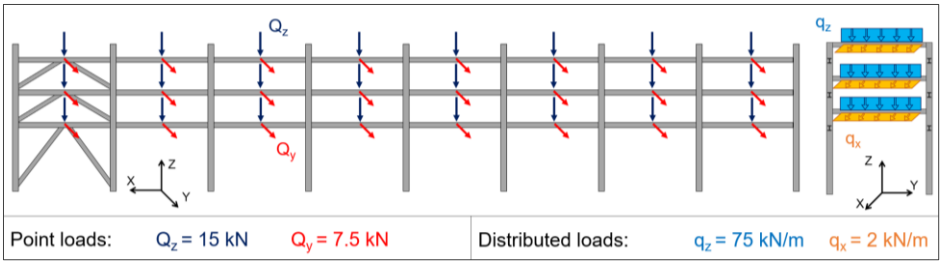

Figure 2. Loads applied on prototype pipe-rack

2.2 Numerical model

The pipe rack described in Section 2.1 was modelled with the thermo-mechanical non-linear finite element software SAFIR [20]. This software includes the LOCAFI model, as described in Section 3.1. The structural response of the pipe-rack exposed to a localised fire was investigated by means of a 3D model that exploited 3D Bernoulli fibre-based beam elements. Thus, at each integration point 2D thermal analyses were performed with heat flux boundary conditions obtained from the application of the LOCAFI model. The entire structure was discretized with beam elements having length of 50 cm and containing two points of integration each. That represents a total of 936 beam elements to model the prototype pipe-rack. The properties of steel at elevated temperature were taken as the ones provided in EN 1993-1-2 [21]. The boundaries conditions assigned to the structural model comply with the assumptions formulated in Section 2.1. As described in Figure 3, the columns HEA340 are continuous and pinned at their base in both principal directions. The transversal beams HEA- and HEB300 are both end fixed to the columns, while the longitudinal beams, HEA200 are pinned to the columns. At both longitudinal ends of the pipe-rack, horizontal restraints were applied to allow for the bracing system that was not modelled to limit the computational burden. This modelling was justified by the fact that based on the fire scenarios described in Section 3.2, the heating of the bracing system was not enough to significantly change its degree of restraint. Moreover, the major thermal impact and the consequent structural failure occurred in the transverse direction. It may be noted that longitudinal thermal expansion joints were not considered in the structural module under study.

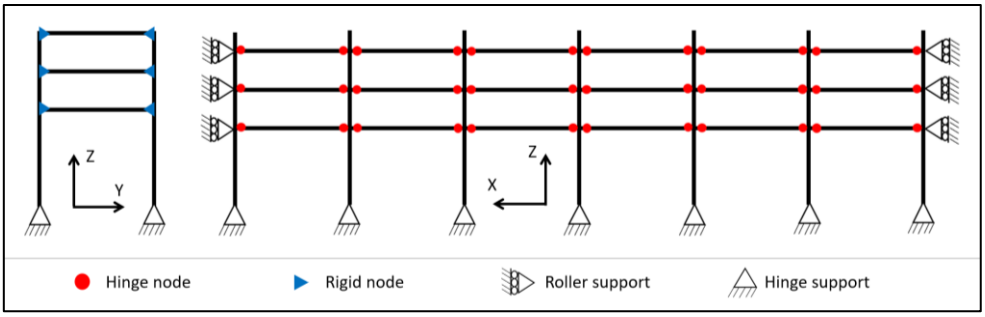

Figure 3. Boundary conditions of the 3D FE model of the prototype steel pipe-rack

3 LOCALISED FIRE SCENARIOS

In this work, emphasis was put on the thermal demand, whose definition for this case study is highly uncertain. Thus, for the derivation of the fire fragility curves, only the uncertainty related to the fire input was considered, but of course other forms of uncertainty can be found, e.g. steel mechanical properties, steel thermal properties, applied loads [15],[16],[22],[23].

3.1 LOCAFI Model

Localised fires results from a liquid or solid fuel burning on a limited surface. Several models are available in literature to study localised fires and they can be classified among field/computational fluid dynamics (CFD) models and empirical/analytical models. Tondini et al. [10] showed how the analytical LOCAFI model compared with CFD models to predict the radiant heat flux emitted from localised fires and how it fared against experimental measurements. Among empirical/analytical models, solid flame models adopt a specific shape for the flame geometry, that may be a cylinder, an elliptical cylinder or a cone [24],[10]. These models consider that the radiative heat fluxes are emitted from the surfaces of the solid representing the fire and that the radiative heat flux received by an external element is the sum of the radiative heat fluxes emitted from each surface based on the computation of configuration factor, which may be done analytically and/or numerically depending on the flame shape assumption. In the framework of this research, a solid flame model is adopted with the use of the LOCAFI model developed within the European LOCAFI Project [9]. This model was developed and calibrated based on experimental tests and numerical analyses performed with a CFD model [10] and it is based on the existing localised fire correlations provided in Annex C of EN1991-2 [25]. Once a localised fire is defined with a conical shape and a temperature evolution along the flame axis, incident radiative heat fluxes can be computed for any external element considered. Equation (1) defines the incident radiative heat flux $\dot{q}_{A\to B}$ emitted by a surface A and received by a surface B.

$$\dot{q}_{A\to B} = \phi_{A\to B}\, \varepsilon_A\, \sigma\, (\theta_A + 273)^4 \qquad [W/m^2] \qquad (1)$$

Where $\phi_{A\to B}$ is the configuration factor, ε_A is the emissivity of the surface A, σ is the Stefan-Boltzmann constant and θ_A is the temperature of the surface A. In this research context, as depicted in Figure 4a, the surface A is an element discretising the conical fire and the surface B is an element discretising the structural steel members. The emissivity of the flame ε_A, or ε_f, is conservatively taken equal to 1. The configuration factor can be determined analytically, if available, otherwise through numerical integration. The configuration factor is calculated considering sizes and orientations of surfaces A and B and the distance separating them. This calculation complexity is function of the discretization level adopted for the fire and for the structure. Two models are available to compute the radiative heat fluxes impacting a structural element; the analytical model [10] and the numerical model [20]. In this work, the model implemented in SAFIR is based on numerical integration of the configuration factor. It discretizes the surfaces of the fire and the member with small elements, as shown in Figure 4b. SAFIR is able to compute at each time step and for each finite element located on the border of the cross section, as depicted in Figure 4c, an incident radiative heat flux that is calculated by summing all the radiative heat fluxes emitted by the surfaces discretizing the fire and visible by the element according to a numerical procedure. Then, the net heat flux is expressed as the difference between the absorbed radiative heat flux and the heat fluxes reemitted by the surface B through radiation and convection, as shown in Equation (2), where the first term is the absorbed radiative heat flux by the surface, the second and third terms are the heat fluxes reemitted by the surface through radiation and convection at ambient temperature, i.e. 20°C.

$$\dot{q}_{net} = \varepsilon_B\, \dot{q}_{A\to B} - \varepsilon_B\, \sigma\, [(\theta_B + 273)^4 - 293^4] - \alpha_c\, (\theta_B - 20) \qquad [W/m^2] \qquad (2)$$

As an example, Figure 4d shows the temperature field observed within the cross section of an HEA340 steel column at a height of 5 m after 1 h of exposure to a heptane localised fire characterised by a diameter of 20 m and located 2 m away.

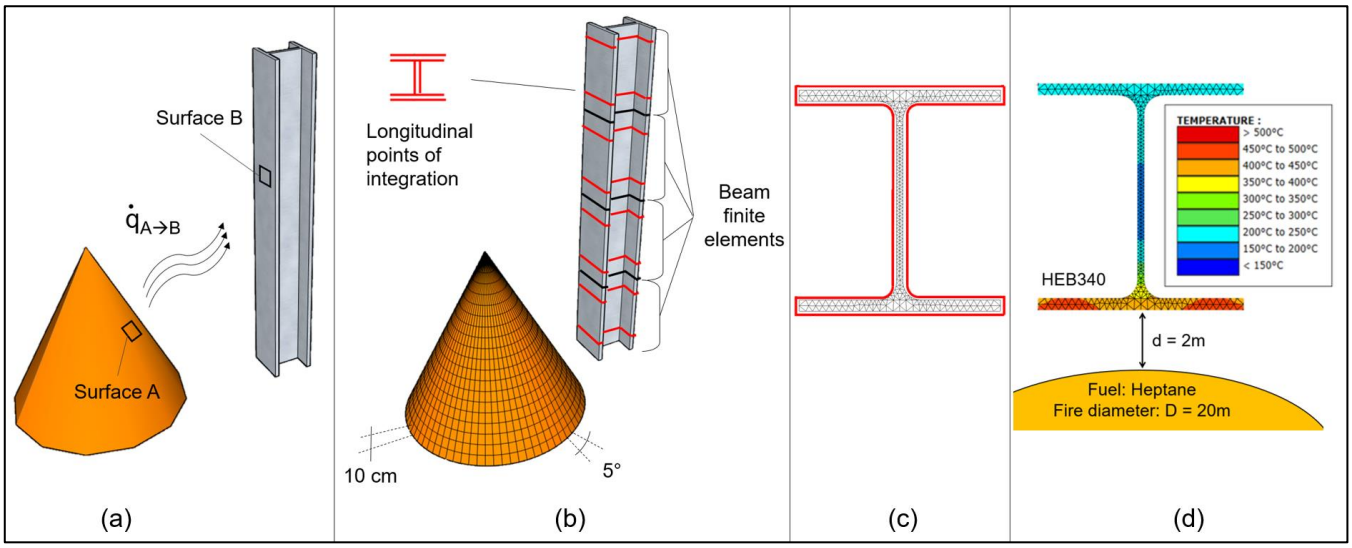

Figure 4. (a) Steel column exposed to localised fire; (b) LOCAFI numerical model; (c) Cross-section discretization; (d) Temperature field within the cross section observed with numerical model

3.2 Selection of fire scenarios

To study the behaviour of the steel pipe-rack exposed to localised fires in a probabilistic way, a meaningful set of fire scenarios must be defined. The objective is to encompass plausible fire scenarios, that impact the structure with different levels of intensity. It was decided to define fire scenarios by varying three parameters: the pool fire diameter, the fuel and the fire-structure distance. As analysed by Randaxhe et al [26], in petrochemical plants, pool fires can result from the ignition of a fuel contained in a cylindrical tank or from the ignition of a leaking fuel. Resulting fires are likely to present a diameter varying between 5m and 30m. Therefore, 11 fire diameters, denoted D, varying between 5 m to 30 m with a step of 2.5 m were selected. Since petrochemical plants deal with various flammable products, 7 liquid fuels were selected to cover a wide range of different fire loads. These 7 fuels are namely listed in Table 1 that defines 77 different localised fires and summarizes the rate of heat release (RHR) computed for each of them.

Table 1. Rate of heat release depending on fuels and fire diameters

Fuel	Rate of heat release [MW]										
	Diameters [m]										
	5	7.5	10	12.5	15	17.5	20	22.5	25	27.5	30
Pentane	91	205	364	569	819	1115	1456	1843	2276	2754	3277
Heptane	71	160	284	443	638	869	1135	1436	1773	2146	2554
Benzene	67	151	268	418	602	820	1071	1355	1673	2025	2409
Kerosene	53	120	213	332	479	652	851	1077	1330	1609	1915
Gasoline	47	106	189	295	425	578	755	956	1180	1428	1699
Fuel Oil	26	60	106	166	239	325	424	537	663	802	954
Acetone	19	43	77	120	173	236	308	390	481	582	693

As explained in Section 3.1, the distance separating a structure and a fire has a direct influence on the magnitude of the radiative heat flux received by the structure. For the definition of the fire scenarios, 7 distances separating the edge of the fire and the structure. The 7 distances, denoted d, are: 0.5 m, 1 m, 2 m, 3 m, 4 m, 5 m and 6 m. It has to be noted that the localised fires were positioned on the axis of the central moment resisting frame in order to have the most important impact on the structure. Fire scenarios with distances d close to 0 m have a significant impact on the structure while the ones close to 6m are definitely less demanding, which explains why no further distance was considered. Eventually, by varying the values of the three parameters: fire diameter, fuel, and distance, 539 fire scenarios were defined and 539 thermo-mechanical analyses with the LOCAFI localised fire model as thermal input were performed in SAFIR.

4 PPROBABILISTIC FIRE DEMAND ANALYSIS

4.1 Cloud analysis method

A fragility function expresses the probability that an engineering demand parameter (EDP) exceeds a structural limit state (LS) as a function of an intensity measure (IM). That probability is usually written in the following form.

$$P(EDP > LS|IM) \quad (3)$$

The aim is to develop fire fragility functions to be used in a probabilistic framework that will serve as a means for practitioners to probabilistically assess/design a pipe-rack structure subjected to localised fires. To build up fragility functions and to define the probability expressed in Equation (3), it is necessary to develop a probabilistic demand model. In literature, several probabilistic seismic demand models (PSDM) can be found, whereas only few probabilistic fire demand models (PFDM) have been developed so far [15-18]. Most PSDMs characterise the relation between EDP and IM based on results obtained through non-linear dynamic analysis. In the framework of this research, the cloud analysis (CA) method appeared to be the most appropriate for the development of a probabilistic fire demand model. In the CA all fire scenarios are run and based on thermo-mechanical results a cloud of points is plotted on an EDP vs IM chart. Assuming that the EDP follows a lognormal distribution when conditioned on the IM, which is a common assumption, it is possible to write the median EDP, i.e. $\widehat{EDP}$, as expressed in Equation (4). Therefore, the conditional median of EDP given IM is linear in log-log space, as shown in Equation (5), whereas the conditional dispersion of EDP given IM is constant. Thus, the resulting probabilistic demand model can be represented in linear and logarithmic forms as in Equations (4) and (5), respectively, where a = exp(A) and b = B. A and B are parameters that can be determined from linear regression. With coefficients a and b, the standard deviation of the linear regression error can be defined with Equation (6). This term is also defined $\beta_{EDP|IM}$ as the dispersion of the EDP conditioned on IM. Considering the lognormal assumption and Equations (4) and (6), Cornell et al. [27] defined the fragility function with the use of a lognormal cumulative distribution function as expressed in Equation (7).

$$\widehat{EDP} = a\ IM^b \quad (4)$$

$$\ln(\widehat{EDP}) = A + B\ln(IM) \quad (5)$$

$$\sigma_{\ln(EDP)|IM} = \beta_{EDP|IM} = \sqrt{\frac{\sum_{i=1}^{n}\left[\ln(EDP_i) - \ln(\widehat{EDP}_i)\right]^2}{n-2}} \quad (6)$$

$$P(EDP > LS|IM) = 1 - \Phi\left(\frac{\ln(LS/(a\ IM^b))}{\beta_{EDP|IM}}\right) \quad (7)$$

Eventually, different EDP-IM pairs can be considered and for each of them fire fragility functions can be derived considering different LS. Therefore Sections 4.2 and 4.3 aim at identifying relevant IMs and EDPs to build PFDMs through CA.

4.2 Intensity measures

An intensity measure (IM) aims at characterising the severity of a fire scenario. Thus, 7 IMs are here proposed in Table 2 to characterise in an efficient way the impact of the localised fire. 3 IMs are the parameters defining the fire scenarios, i.e. D, d and q, while 4 IMs are functions of them. The parameter q is referred to as the RHR density. That is appropriate to characterise the power associated to a fuel. The fire position L in the ratio L/D corresponds to the distance separating the structure from the centre of the fire and it is simply derived from distance d and fire diameter D. The maximum average radiative heat flux impinging the structure HF_{avg} considered here as IM was evaluated for each of the 539 fire scenarios with the analytical LOCAFI model [10]. It was computed as the weighted average heat flux impinging the four sides of the cross section impinged by maximum radiative heat flux computed with the LOCAFI model.

Table 2. Intensity measures

IM	Name	Unit	Function
D	Fire diameter	m	f(D)
d	Structure fire distance	m	f(d)
q	Equivalent RHR density of the fuel	MW/m²	f(q)
L/D	Fire position-fire diameter ratio	-	f(D,d)
L_{Fl}	Flame length	m	f(D,q)
HF_{avg}	Maximum average heat flux impinging the structure	kW/m²	f(D,d,q)
d/L_{Fl}	Structure fire distance - flame length ratio	-	f(D,d,q)

4.3 Engineering demand parameters

The selection of appropriate engineering demand parameters (EDP) that are able to describe the structural response is paramount to build a probabilistic demand model. Thus, in order to identify suitable EDPs considering localised fire located beside the structure, 130 analyses out of the 539 scenarios, were deeply investigated. These 130 cases are among the ones causing major internal actions and displacements. For 59 cases, the structure failed within 60 minutes of analysis, whereas for the 71 other cases, the structure survived the whole analysis. Based on these analyses, 5 possible EDPs for the case under study were identified and reported in Table 3.

Table 3. Engineering demand parameters

EDP	Name	Unit
ISDR	Interstorey drift ratio	%
N_Z	Axial load	kN
M_X	Bending moment	kNm
T_{MAX}	Maximum average temperature	°C
T_{AVG}	Average temperature	°C

For each of the 130 analyses, ISDR, N_Z and M_X were respectively the maximum interstorey drift ratio, axial load and bending moment observed within the structure. T_{MAX} was the maximum average temperature computed within the whole structure, while T_{AVG} was the average temperature within the highly stressed structural element. These EDPs were evaluated and compared based on their ability to characterise the structural response and it appeared that the ISDR was the most suitable EDP. In fact, it offers several advantages: i) it only considers the structural response, independently from the fire scenario and it is representative of the fire scenarios that cause significant lateral displacement; ii) it is straightforward to evaluate and to compare with other structural and load configurations and iii) it can be associated with specific structural damage states as referred in literature. In this respect, the American seismic rehabilitation prestandard [28] associates, for steel moment resisting frames, an ISDR equal to 5% and an ISDR equal to 2.5% that are representative of a near collapse limit state and life safety limit state, respectively. Differently from the seismic case where the ISDR is widely used as EDP, some care might have to be taken for structural fire applications. Nevertheless, in this study, the ISDR can be assumed as global EDP because it can be related to damage and collapse of a significant part of the pipe-rack. Therefore, ISDR values of 5% and 2.5% were adopted in the probabilistic fire demand model framework as limit states.

4.4 Results of the numerical analyses

As explained in Sections 2.2 and 3.1, numerical analyses were performed with SAFIR. The analyses were run for 60 minutes, a time during which the different structural members received a constant heat flux so that they could reach their thermal equilibrium as for steel temperature. The impact of the localised fire on structural members was investigated for the entire pipe-rack. Figure 5a depicts the pipe-rack after a 60 min exposure to a heptane pool fire characterised by a diameter of 20 m and located 2 m away from the structure. The thermal effect of the localised fire and the horizontal loads applied in the positive y-direction induced significant horizontal displacements. These horizontal displacements increased during the fire owing to thermal bowing and loss of stiffness of steel and consequently second order effects became not negligible.

As expected, the fire scenarios under consideration induced significant non-uniform heating in the cross sections, as shown in Figure 5b and 5c, that depict the temperature fields within the cross sections located at an height of 5 m of columns A4 and A3, that are respectively 2 m and 3.41 m distant from the fire. Among the 539 fire scenarios investigated, 59 cases led the pipe-rack to collapse. In this respect, Figure 5d depicts the failure mechanism of the structure, which involves the loss of stability of the central frame. The displacements were maximal at the top of the structure (9 m high) but the highest interstorey drift ratios (ISDR) were observed transversally at the first level of the columns. Table 4 reports on the maximum ISDRs observed for each of the 539 analyses and provides an overview of the influence of the basic fire parameters D, d and q on the structural response. As expected, the increase in ISDR is generally related to an increase in fire diameter D and/or to a reduction in the fire-structure distance d and/or to a more hazardous fuel in terms of higher mass burning rate or heat of combustion. In Table 4, green cells indicate ISDR values between 2.5% and 5% and red cells indicate values greater than 5%. Based on the 539 results of the numerical analysis, using the ISDR as EDP, and by considering the IM candidates listed in Table 2, PFDMs were developed through CA. For brevity here only the 2 best IM candidates, i.e. HF_{avg} and L/D, will be considered and for a more comprehensive analysis refer to Randaxhe et al.[26].

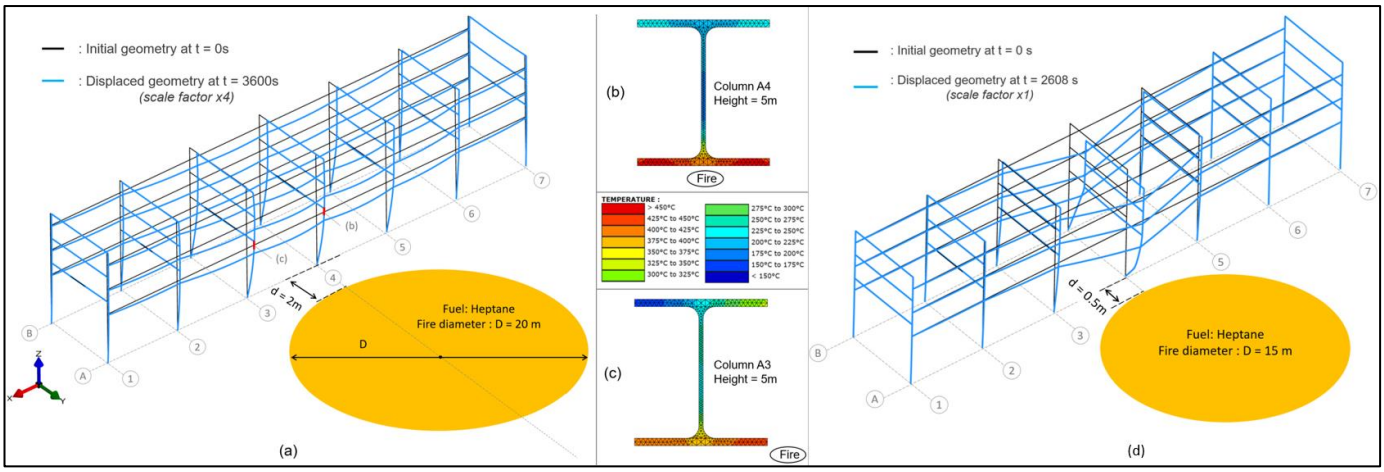

Figure 5. - Steel pipe-rack exposed to fire scenario "D=20m – d=2m – Fuel=Heptane" for 60 min: (a) Initial and displaced shape of the structure; (b) Temperature field in cross section of column A4 (h=5m); (c) Temperature field within in cross section column A3 (h=5m); (d) Steel pipe-rack exposed to fire scenario "D=15m – d=0.5m – Fuel=Heptane": Failure of the structure after 2608 s

4.5 Fire fragility functions

An IM is qualified efficient if it generates low variations between actual and predicted EDP values for a given IM value. That variation is characterised by the dispersion $\beta_{EDP|IM}$ of the EDP conditioned on the IMs, as expressed in Equation (6), which is satisfying when its value is low. Usually a value lower than 0.3 is considered efficient [29]. For both IM candidates, the values of dispersion $\beta_{EDP|IM}$ were computed and reported in Figure 6. Eventually, it appeared that both IM candidates are efficient since they exhibit dispersion values lower than 0.3. In particular, the most efficient candidate IM is the maximum average heat flux imping the structure HF_{avg}. Based on the definition of the probabilistic fire demand models, fragility functions were derived considering the maximum average heat flux impinging the structure HF_{avg} as IM, since it was found to be the most efficient. The ISDR was used as EDP and the two limit states (LS) defined in Section 4.3 were considered. Applying the CA, fragility functions could be derived for both LS using Equation (7). As illustrated in Figure 6a, when HF_{avg} was taken as IM, coefficients a and b were found to be equal to 0.007 and 0.620, respectively, and they yielded the dispersion value $\beta_{EDP|IM}$ of 0.09. Fragility curves are plotted in Figure 7a that show the probability of the interstorey drift ratio ISDR exceeding 5% and 2.5% conditioned on the maximum average heat flux impinging the structure HF_{avg}. These functions can be used to quantify the probability that a steel pipe-rack exposed to localised fire exceeds a predefined LS. It is possible to note that when $HF_{avg} > 30$ kW/m² the probability of exceeding an ISDR value of 5% becomes larger than 80%, whereas it occurs for $HF_{avg} > 10$ kW/m² when considering the life safety limit state, i.e. ISDR = 2.5%.

Table 4. Maximum interstorey drift ratios observed for the 539 fire scenarios

Distance d [m]	Fuels	Interstorey drift ratios										
		Fire diameters D [m]										
		5	7.5	10	12.5	15	17.5	20	22.5	25	27.5	30
6	Pentane	1.79%	2.43%	2.89%	3.21%	3.43%	3.58%	3.70%	3.77%	3.83%	3.87%	3.90%
6	Heptane	1.68%	2.31%	2.77%	3.10%	3.33%	3.49%	3.62%	3.70%	3.77%	3.81%	3.85%
6	Benzene	1.66%	2.27%	2.74%	3.07%	3.30%	3.47%	3.60%	3.68%	3.75%	3.80%	3.84%
6	Kerosene	1.56%	2.14%	2.61%	2.95%	3.19%	3.36%	3.49%	3.59%	3.67%	3.72%	3.77%
6	Gasoline	1.51%	2.07%	2.53%	2.87%	3.11%	3.29%	3.42%	3.53%	3.61%	3.67%	3.72%
6	Fuel Oil	1.27%	1.69%	2.09%	2.40%	2.65%	2.84%	2.98%	3.10%	3.19%	3.26%	3.32%
6	Acetone	1.16%	1.48%	1.81%	2.09%	2.31%	2.48%	2.62%	2.73%	2.81%	2.88%	2.94%
5	Pentane	2.03%	2.71%	3.16%	3.46%	3.66%	3.79%	3.88%	3.93%	3.96%	4.00%	4.04%
5	Heptane	1.91%	2.58%	3.04%	3.35%	3.57%	3.71%	3.81%	3.87%	3.92%	3.96%	4.00%
5	Benzene	1.88%	2.55%	3.01%	3.32%	3.54%	3.69%	3.79%	3.86%	3.90%	3.94%	3.99%
5	Kerosene	1.76%	2.41%	2.88%	3.20%	3.43%	3.59%	3.70%	3.78%	3.83%	3.88%	3.92%
5	Gasoline	1.70%	2.33%	2.80%	3.13%	3.36%	3.53%	3.64%	3.73%	3.79%	3.83%	3.88%
5	Fuel Oil	1.40%	1.91%	2.33%	2.66%	2.90%	3.08%	3.21%	3.32%	3.40%	3.46%	3.52%
5	Acetone	1.25%	1.65%	2.02%	2.32%	2.55%	2.72%	2.85%	2.95%	3.03%	3.09%	3.14%
4	Pentane	2.33%	3.00%	3.44%	3.73%	3.90%	4.00%	4.05%	4.08%	4.11%	4.25%	4.32%
4	Heptane	2.20%	2.88%	3.33%	3.63%	3.82%	3.94%	4.00%	4.04%	4.08%	4.11%	4.20%
4	Benzene	2.16%	2.85%	3.30%	3.61%	3.80%	3.92%	3.99%	4.03%	4.06%	4.09%	4.16%
4	Kerosene	2.03%	2.71%	3.17%	3.49%	3.70%	3.83%	3.91%	3.96%	4.01%	4.04%	4.07%
4	Gasoline	1.95%	2.63%	3.09%	3.41%	3.63%	3.77%	3.86%	3.92%	3.97%	4.00%	4.04%
4	Fuel Oil	1.57%	2.17%	2.61%	2.94%	3.18%	3.34%	3.46%	3.55%	3.62%	3.67%	3.72%
4	Acetone	1.38%	1.87%	2.28%	2.58%	2.81%	2.98%	3.10%	3.19%	3.26%	3.32%	3.36%
3	Pentane	2.66%	3.33%	3.76%	4.03%	4.17%	4.21%	4.22%	4.28%	4.54%	4.68%	4.86%
3	Heptane	2.53%	3.21%	3.66%	3.94%	4.10%	4.16%	4.19%	4.20%	4.35%	4.49%	4.62%
3	Benzene	2.50%	3.18%	3.63%	3.91%	4.07%	4.15%	4.18%	4.19%	4.31%	4.44%	4.58%
3	Kerosene	2.35%	3.04%	3.50%	3.80%	3.98%	4.07%	4.12%	4.15%	4.16%	4.27%	4.40%
3	Gasoline	2.27%	2.96%	3.42%	3.73%	3.92%	4.02%	4.08%	4.12%	4.14%	4.17%	4.30%
3	Fuel Oil	1.81%	2.47%	2.93%	3.25%	3.48%	3.63%	3.72%	3.80%	3.85%	3.89%	3.92%
3	Acetone	1.56%	2.14%	2.57%	2.89%	3.11%	3.26%	3.37%	3.46%	3.51%	3.56%	3.60%
2	Pentane	3.02%	3.69%	4.15%	4.40%	4.46%	4.41%	4.47%	5.02%	5.39%	5.31%	5.54%
2	Heptane	2.89%	3.57%	4.04%	4.31%	4.40%	4.39%	4.35%	4.70%	5.10%	5.56%	5.45%
2	Benzene	2.85%	3.53%	4.00%	4.28%	4.38%	4.38%	4.34%	4.63%	5.00%	5.31%	5.34%
2	Kerosene	2.71%	3.39%	3.87%	4.16%	4.30%	4.33%	4.32%	4.29%	4.68%	4.86%	4.89%
2	Gasoline	2.62%	3.31%	3.79%	4.09%	4.24%	4.29%	4.30%	4.28%	4.53%	4.70%	4.74%
2	Fuel Oil	2.12%	2.81%	3.28%	3.61%	3.82%	3.94%	4.02%	4.07%	4.10%	4.13%	4.16%
2	Acetone	1.81%	2.45%	2.90%	3.22%	3.44%	3.59%	3.68%	3.76%	3.81%	3.85%	3.89%
1	Pentane	3.37%	4.10%	4.65%	5.33%	4.96%	4.55%	5.47%	5.29%	5.28%	5.27%	5.27%
1	Heptane	3.24%	3.97%	4.51%	4.86%	4.84%	4.58%	5.27%	5.41%	5.20%	5.38%	5.41%
1	Benzene	3.20%	3.93%	4.47%	4.81%	4.81%	4.59%	5.09%	5.31%	5.26%	5.19%	5.20%
1	Kerosene	3.06%	3.79%	4.32%	4.64%	4.72%	4.59%	4.67%	5.37%	5.37%	5.24%	5.33%
1	Gasoline	2.97%	3.70%	4.23%	4.56%	4.66%	4.58%	4.48%	5.16%	5.38%	5.40%	5.30%
1	Fuel Oil	2.46%	3.16%	3.67%	4.03%	4.24%	4.32%	4.34%	4.33%	4.32%	4.57%	4.67%
1	Acetone	2.09%	2.77%	3.26%	3.60%	3.83%	3.97%	4.04%	4.09%	4.12%	4.12%	4.14%
0.5	Pentane	3.50%	4.28%	5.35%	5.14%	5.10%	5.50%	5.39%	5.39%	5.23%	5.06%	5.45%
0.5	Heptane	3.38%	4.15%	4.88%	5.16%	5.13%	4.77%	5.39%	5.34%	5.09%	5.33%	5.40%
0.5	Benzene	3.34%	4.11%	4.81%	5.27%	5.14%	4.67%	5.23%	5.12%	5.32%	5.25%	5.19%
0.5	Kerosene	3.20%	3.97%	4.58%	5.34%	5.25%	4.62%	5.43%	5.32%	5.25%	5.36%	5.53%
0.5	Gasoline	3.12%	3.88%	4.48%	4.95%	5.01%	4.64%	4.39%	5.31%	5.40%	5.22%	5.43%
0.5	Fuel Oil	2.60%	3.34%	3.89%	4.26%	4.45%	4.48%	4.44%	4.39%	4.77%	5.07%	5.58%
0.5	Acetone	2.23%	2.93%	3.44%	3.81%	4.03%	4.15%	4.20%	4.22%	4.21%	4.21%	4.19%

Finally, fragility curves considering L/D as IM were also derived and plotted in Figure 7b, because it is an IM commonly used in practice. Furthermore, the L/D IM was found to be the most efficient and sufficient after the maximum average heat flux impinging the structure HF_{avg} [26]. The PFDM provided, through linear regression a and b coefficients to be equal to 0.026 and -0.976 and dispersion $\beta_{EDP|IM}$ equal to 0.13, as illustrated in Figure 6b. It can be observed that these fragility curves are meaningful if $L/D \geq 0.5$, because when the L/D decreases below 0.5 it means that part of the structure is engulfed into the localised fire and consequently a different structural response is expected with the ISDR no longer being the most appropriate EDP. Therefore, a grey shade for L/D values < 0.5 was included in Figure 7b to highlight the validity range of the fire fragility curves. It may be observed that when L/D is larger than 0.75 the probability of exceeding an ISDR value of 5% becomes very low and only from L/D < 0.75 the probability increases. For L/D = 0.5 it attains almost 60%. When L/D > 1.5 the probability of exceeding an ISDR = 2.5% becomes almost zero, whereas it overcomes 80% when L/D < 0.9.

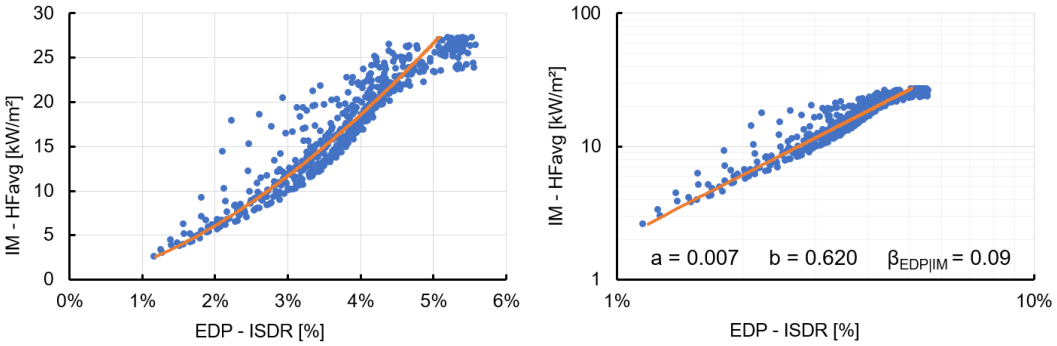

(a)

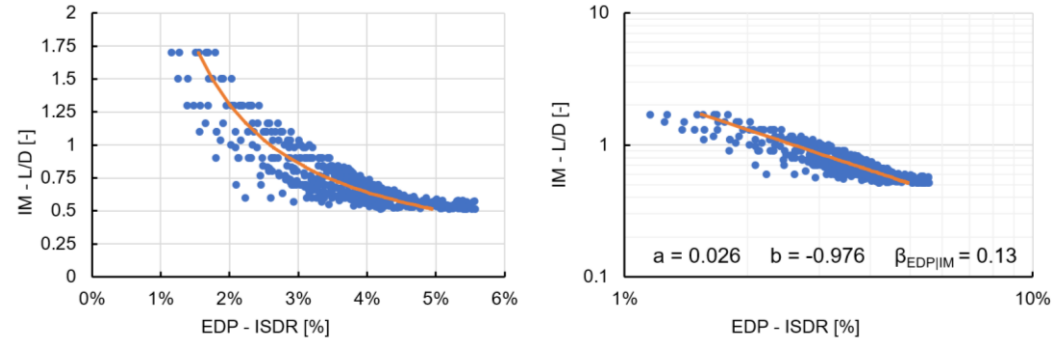

(b)

Figure 6. Cloud analysis and linear regression for IMs: (a) HF_{avg}; (b) L/D

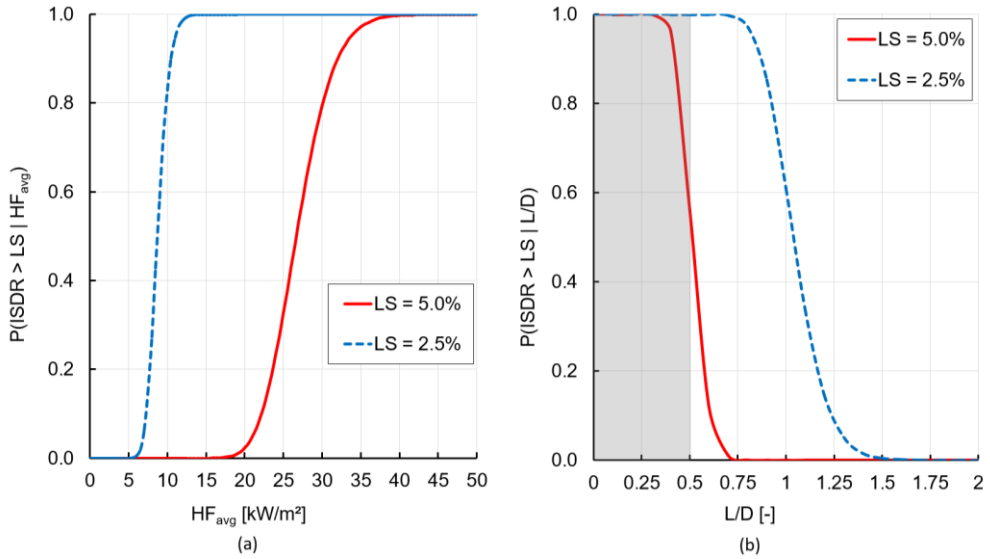

Figure 7. (a) Fragility curves based on CA for near collapse- and life safety preventions with HFavg as IM; (b) Fragility curves based on CA for near collapse- and life safety preventions with L/D as IM

5 CONCLUSION

This paper presented the development of a probabilistic fire demand model for a steel pipe-rack exposed to localised fires. Considering 539 localised plausible fire scenarios in industrial/petrochemical plants, thermo-mechanical analyses were performed with the FE software SAFIR that includes the LOCAFI localised fire model. Based on numerical analyses, probabilistic analyses were conducted to derive fire fragility functions by adopting the cloud analysis (CA) method. The maximum transversal interstorey drift ratio (ISDR) was found to be the most suitable EDP for this case study, because it provides a global measure of the structural response as it can be related to damage and collapse of a significant part of the pipe rack. In this respect, two structural ultimate limit states, near collapse and life safety, were defined for ISDR exceeding 5% and 2.5%, respectively. Two intensity measures (IM) were here considered and compared based on their efficiency. The maximum average heat flux impinging the structure HF_{avg} and the ratio between fire position and fire diameter L/D appeared to be efficient IMs to characterise the localised fire severity. Thus, fire fragility functions were derived considering these two EDP-IM pairs, i.e. ISDR-HF_{avg} and ISDR-L/D. Focusing on the near collapse limit state, fragility functions showed that localised fires generating HF_{avg} lower than 20 kW/m² have low probability of exceedance. Conversely, when HF_{avg} is higher than 35 kW/m², it is close to 1. For L/D values higher than 0.75 the probability of exceedance an ISDR of 5% is very low. Regarding the life safety limit state, fragility functions showed for HFavg higher than 15 kW/m² the probability of exceedance is very high, as well as when the L/D value varies between 0.5 and 0.75. In sum, the CA can be considered an appropriate and versatile method to develop PFDMs from which building fire fragility functions to be used in fire risk assessment or in a fully probabilistic structural fire engineering (PSFE) framework of steel pipe-rack design. Future works will be addressed to consider the uncertainty in the structural capacity, multiple burning pool fires and the presence of the wind.

ACKNOWLEDGMENTS

This research has been funded by the European H2020 Marie Skłodowska- Curie XP-RESILIENCE project through the grant agreement number 721816. This work was also supported by the Italian Ministry of Education, University and Research (MIUR) in the frame of the 'Departments of Excellence' (grant L 232/2016).

REFERENCES

1. Zheng B, Chen G. Storage Tank Fire Accidents. *Process Saf Prog*. 2011;30(3). doi:10.1002/prs
2. Chang JI, Lin C. A study of storage tank accidents. *J Loss Prev Process Ind*. 2005;19:51-59. doi:10.1016/j.jlp.2005.05.015
3. Pantousa D. Thin-Walled Structures Numerical study on thermal buckling of empty thin-walled steel tanks under multiple pool- fi re scenarios. *Thin Walled Struct*. 2018;131(January):577-594. doi:10.1016/j.tws.2018.07.025
4. F.Paolacci, O.Bursi, Md.S.Reza, A.Kumar, A.M.Gresnigt. Main Issues On The Seismic Design Of Industrial Piping Systems And Components. In: *ASME 2013 Pressure Vessels & Piping Division Conference*. ; 2013:1-10.
5. Paolacci F. Structural safety of industrial steel tanks; pressure vessels and piping - Basic seismic structural design of a typical piping system. 2010;(February 2010).
6. Bursi O, Paolacci F, Reza MS, Alessandri S, Tondini N. Seismic Assessment of Petrochemical Piping Systems Using a Performance-Based Approach. *J Press Vessel Technol*. 2010.
7. Paolacci F, Bursi OS, Md.Shahin R. SEISMIC ANALYSIS AND COMPONENT DESIGN OF REFINERY. In: *Conference on Computational Methods in Structural Dynamics and Earthquake Engineering*. ; 2011:26-28.
8. Bursi OS, Paolacci F, Reza MS. Performance-Based Analysis of Coupled Support Structures and Piping Systems. In: *ASME 2015 Pressure Vessels & Piping Division Conference*. ; 2015. doi:10.1115/PVP2015-45123
9. Francis P, Baddo N, Hanus F, Thauvoye C. Design of columns subject to localised fires. 2018.
10. Tondini N, Thauvoye C, Hanus F, Vassart O. Development of an analytical model to predict the radiative heat flux to a vertical element due to a localised fire. *Fire Saf J*. 2019;105(March):227-243. doi:10.1016/j.firesaf.2019.03.001

11. Kamikawa D, Hasemi Y, Wakamatsu T, Kagiya K. Experimental flame heat transfer correlations for a steel column adjacent to and surrounded by a pool fire. In: *Fire Safety Science - Seventh International Symposium*. ; 2000:989-1000.
12. Santiago A, Ferraz G, Rodrigues JP, Barata P. Thermal analysis of hollow steel columns exposed to localised fires. *Fire Technol*. 2016;52:663-681. doi:10.1007/s10694-015-0481-2
13. Hanus F, Vassart O, Tondini N, Nadjai A, Franssen J. Temperature assessment of a vertical steel member subjected to localised fire: Experimental tests. In: *Proceedings of the 9th Conference on Structures in Fire*. Princeton (NJ) USA; 2016.
14. Tondini N, Franssen J-M. Analysis of experimental hydrocarbon localised fires with and without engulfed steel members. *Fire Saf J*. 2017;92(May):9-22. doi:10.1016/j.firesaf.2017.05.011
15. Gernay T, Khorasani NE, Garlock M. Fire fragility curves for steel buildings in a community context : A methodology. *Eng Struct*. 2016;113:259-276. doi:10.1016/j.engstruct.2016.01.043
16. Gernay T, Khorasani NE, Garlock M. Fire Fragility Functions for Steel Frame Buildings: Sensitivity Analysis and Reliability Framework. *Fire Technol*. 2019;55(4):1175-1210. doi:10.1007/s10694-018-0764-5
17. Lange D, Devaney S, Usmani A. An application of the PEER performance based earthquake engineering framework to structures in fire. *Eng Struct*. 2014;66:100-115.
18. Shrivastava M, Abu AK, Dhakal RP, Moss PJ. Severity measures and stripe analysis for probabilistic structural fire engineering. *Fire Technol*. 2019;55(4):1147-1173. doi:10.1007/s10694-018-0799-7
19. Cornell CA, Krawinkler H. Progress and challenges in seismic performance assessment. *Peer Cent News*. 2000;3(2):1-3.
20. Franssen JM, Gernay T. Modeling structures in fire with SAFIR®: Theoretical background and capabilities. *J Struct Fire Eng*. 2017;8(3):300-323. doi:10.1108/JSFE-07-2016-0010
21. European Committee for Standardization CEN. Eurocode 3: Design of steel structures – Part 1–2: General rules – structural fire design. EN 1993-1-2. 2005.
22. Khorasani NE, Gardoni P, Garlock M. Probabilistic Fire Analysis: Material Models and Evaluation of Steel Structural Members. *J Struct Eng*. 2015;141(12). doi:10.1061/(ASCE)ST.1943-541X.0001285
23. Qureshi R, Ni S, Elhami Khorasani N, Van Coile R, Hopkin D, Gernay T. Probabilistic Models for Temperature-Dependent Strength of Steel and Concrete. *J Struct Eng*. 2020;146(6). doi:10.1061/(ASCE)ST.1943-541X.0002621
24. Shokri M, Beyler CL. Radiation from large pool fires. *SFPE Handb Fire Prot Eng*. 1989;4(1):141-150.
25. European Commitee for Standardization C. Eurocode 1: Actions on structures – Part 1–2: General actions – actions on structures exposed to fire. EN 1991-1-2. 2002.
26. Randaxhe J, Popa N, Tondini N. Probabilistic fire demand model for steel pipe-racks exposed to localised fires. *Eng Struct*. 2021;226(March 2020). doi:10.1016/j.engstruct.2020.111310
27. Cornell CA, Jalayer F, Hamburger RO, Foutch DA. Probabilistic Basis for 2000 SAC Federal Emergency Management Agency Steel Moment Frame Guidelines. *J Struct Eng*. 2002;(April):526-533. doi:10.1061/(ASCE)0733-9445(2002)128
28. FEMA, ASCE. FEMA 356 - Prestandard and commentary for the seismic rehabilitation of buildings. 2000;(November).
29. Tondini N, Stojadinovic B. Probabilistic seismic demand model for curved reinforced concrete bridges. *Bull Earthq Eng*. 2012. doi:10.1007/s10518-012-9362-y